Chemical Exchange Saturation Transfer MRI: What Neuro-Oncology Clinicians Need To Know

Pejman Jabehdar Maralani, MD, FRCPC[1,2] (iD), Rachel W. Chan, PhD[2], Wilfred W. Lam, DPhil[2], Wendy Oakden, PhD[2], Ryan Oglesby, PhD[3] (iD), Angus Lau, PhD[2,3], Hatef Mehrabian, PhD[2], Chris Heyn, MD, PhD[1], Aimee K.M. Chan, MSc[2], Hany Soliman, MD[4], Arjun Sahgal, MD[4], and Greg J. Stanisz, PhD[2,3]

Abstract

Chemical exchange saturation transfer (CEST) is a relatively novel magnetic resonance imaging (MRI) technique with an image contrast designed for in vivo measurement of certain endogenous molecules with protons that are exchangeable with water protons, such as amide proton transfer commonly used for neuro-oncology applications. Recent technological advances have made it feasible to implement CEST on clinical grade scanners within practical acquisition times, creating new opportunities to integrate CEST in clinical workflow. In addition, the majority of CEST applications used in neuro-oncology are performed without the use gadolinium-based contrast agents which are another appealing feature of this technique. This review is written for clinicians involved in neuro-oncologic care (nonphysicists) as the target audience explaining what they need to know as CEST makes its way into practice. The purpose of this article is to (1) review the basic physics and technical principles of CEST MRI, and (2) review the practical applications of CEST in neuro-oncology.

Introduction

The basis of chemical exchange saturation transfer (CEST) was first described in 1963,[1] but it was not until 2000 when the results of the first CEST magnetic resonance (MR) experiment were published.[2] Since then, a significant number of preclinical and clinical studies have demonstrated the potential utility of CEST MR imaging (MRI), alongside major technical developments, which have rendered it clinically feasible.[3]

The main advantage of CEST is its ability to measure in vivo metabolites of interest that may have low concentrations and can alter during different disease processes. Although some CEST applications use exogenous contrast agents[4,5]

[1] Department of Medical Imaging, University of Toronto, Toronto, ON, Canada
[2] Physical Sciences, Sunnybrook Research Institute, Toronto, ON, Canada
[3] Department of Medical Biophysics, University of Toronto, Toronto, ON, Canada
[4] Department of Radiation Oncology, University of Toronto, Toronto, ON, Canada

Corresponding Author:
Pejman Jabehdar Maralani, MD, FRCPC, Department of Medical Imaging, Sunnybrook Health Sciences Centre, 2075 Bayview Avenue, Room AG270c, Toronto, ON, M4N3M5, Canada.
Email: pejman.maralani@sunnybrook.ca

and represent very relevant applications of CEST, many CEST applications in neuro-oncologic imaging do not require exogenous contrast agents such as gadolinium-based contrast agents.

Owing to higher spatial resolution and improved sensitivity to certain low-concentration metabolites compared to proton MR spectroscopy (MRS) methods,[6] there has been a dramatic increase in new and emerging CEST methods in the recent decade and growing clinical translation of these methods, particularly for neuro-oncological applications.[3] The purpose of this paper is to provide an overview that is accessible to a clinical neuro-oncological audience and to briefly summarize recent research in areas of unmet need in neuro-oncology.

Basic Physics of CEST

Chemical Shift

Hydrogen nuclei (or simply, "protons") bonded to metabolites have a different precession frequency than those protons in water molecules, because of changes in the local magnetic field due to electron shielding. This phenomenon, referred to as chemical shift (typically defined in parts per million (ppm) or in Hertz, both relative to water in the case of CEST) is what enables techniques such as MRS and CEST to differentiate the signals coming from protons of different metabolites.

Chemical Exchange

CEST imaging also relies on another intrinsic molecular phenomena called chemical exchange, whereby certain protons (eg, within metabolites) can physically switch places with another proton (eg, from nearby water molecules). Exchange is always happening and can occur with rates as high as hundreds or thousands of times per second. Using standard MRI methods, it can be difficult (if not impossible) to directly measure the signal from metabolites due to very low concentrations. However, the continuous exchange of protons with those of water molecules will thereby influence the water signal, which is detectable by standard MRI methods, making it possible to indirectly detect the metabolites.

The first step of a CEST experiment is to use a long radiofrequency (RF) saturation pulse, or pulse train (on the order of seconds), applied at the resonance frequency of protons in the metabolite of interest to "saturate" them. The saturated protons will undergo chemical exchange (ie, physically switch places) with nonsaturated water protons. Immediately following this exchange, the MRI signal detected at the water frequency will decrease, due to the presence of protons that are already saturated (Figure 1). The difference in signal strength with and without the saturation pulse provides an indirect measure of the concentration the chemical group of interest, which could include amide, amine, guanidinium, or hydroxyl groups.
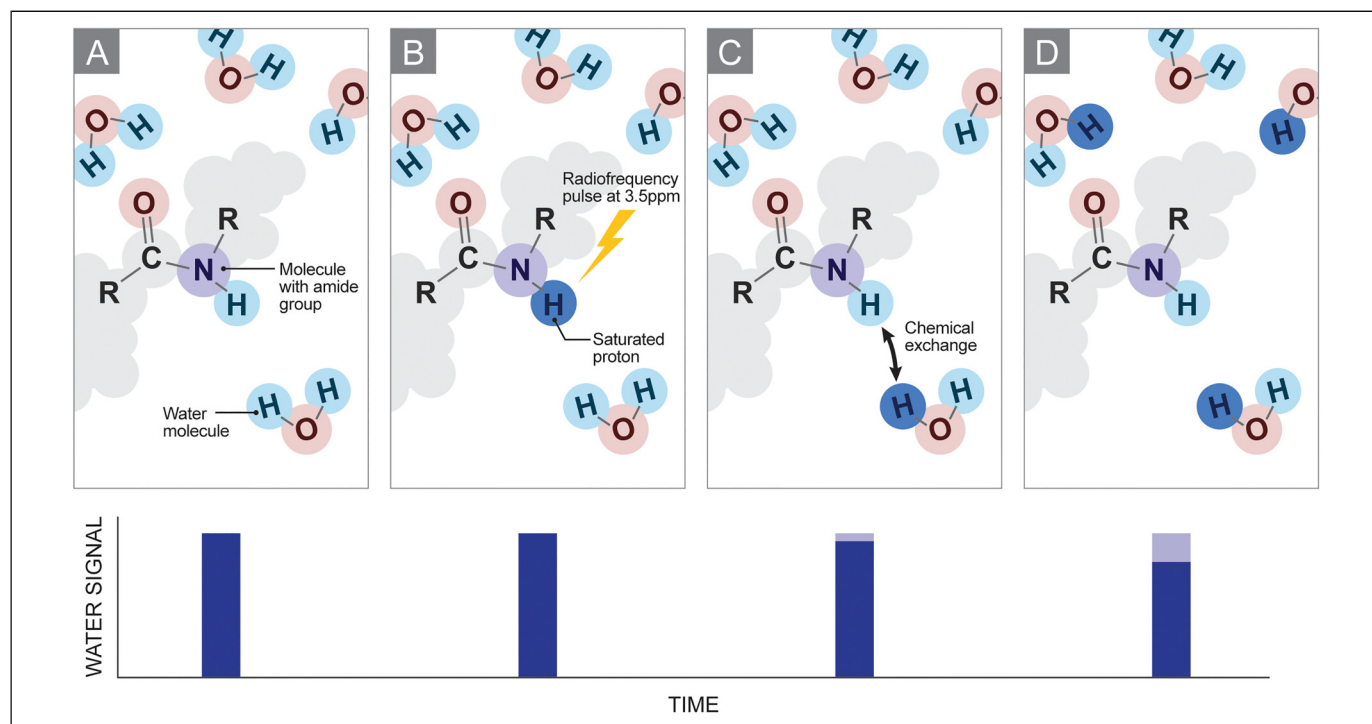

Figure 1. Schematic representation of chemical exchange saturation transfer (CEST): (A-D) Diagrams of the metabolite of interest containing an amide group are shown with surrounding water molecules, for each step in the CEST saturation and exchange process. The water signal level corresponding to each subfigure is shown below each panel. (A) Before saturation. (B) Radiofrequency saturation pulse is applied at a frequency offset of 3.5 ppm relative to water to saturate the proton in the amide group. (C) The saturated proton in the amide group is exchanged with the unsaturated water protons. (D) A continuous exchange of saturated protons leads to a measurable decrease in signal from water.

With sufficient time of RF saturation, a saturation steady state can be achieved providing maximal CEST contrast for the given pulse train. However, reaching a steady state is not always feasible as the duration of the RF pulse is limited by acquisition time, hardware constraints and specific absorption rate (SAR) limitations. As a result, the CEST contrast depends on numerous factors including the concentration of the metabolite of interest, efficiency of saturation, and exchange rate, which itself is dependent on both temperature and pH.[7]

Saturation pulse amplitudes and application duration are important factors for CEST imaging.[8,9] Lower pulse amplitudes and longer durations (≥ 1 s) are used to select chemical groups with slower exchange rate and higher amplitudes and shorter durations for groups with faster exchange rate.[10] The optimal amplitude also depends on the static field strength ($B0$). The consensus for amide proton transfer (APT) weighted brain imaging at 3T is $2\,\mu T$ for 2 s.[3] For the amide CEST peak, which has slower exchange, 1 to 3 μT allows for efficient labelling.[3] For amine, guanidinium, and hydroxyl peaks, which have faster exchange, 2.9 to 12 μT have been used.[10]

Measurement of CEST Signals

As stated above, the CEST contrast depends on the difference in the water signal between images acquired with and without RF saturation pulses at a specific frequency offset. However, there are several other mechanisms that affect the water signal during the saturation process.[11] The two main considerations that need to be taken into account when measuring the CEST signal are magnetization transfer contrast (MTC) and the direct effect of water saturation.

MTC has been used in neuroimaging for several decades and refers to the transfer of magnetization between water and immobile semisolid macromolecules or myelin lipid content such as galactocerebrosides.[12] These semisolid compounds have T2 relaxation times that are too short to be directly measured, while metabolites interrogated by CEST have much longer T2 relaxation times. The exchange rate of saturated protons with water protons is generally, but not always, faster in CEST ($\approx$ 30-5500 Hz)[13] than in MTC ($\approx$ 20-40 Hz).[14] Unlike CEST which is specific to the resonance frequency of protons in a particular metabolite, MTC occurs over a wide range of frequencies. As a result, MTC is less affected by the specific frequency offset.[7]

The direct effect of water saturation relates to the undesired saturation of water protons when intending to saturate protons in a metabolite of interest. This happens because an RF pulse has a nonzero width, so although it is centered on the resonance frequency of the proton of interest, it will directly saturate some water molecule protons. Measuring water signal when saturating protons at the opposite frequency offset ($-\Delta\omega$) can eliminate this and is referred to as the magnetization transfer ratio (MTR) asymmetry (MTR_{asym}). Both the MTR and MTR_{asym} are the most commonly used parameters in CEST are defined as the following:

$$MTR = \frac{S_0 - S_{sat}(\Delta\omega)}{S_0}$$

$$MTR_{asym} = \frac{S_{sat}(-\Delta\omega) - S_{sat}(\Delta\omega)}{S_0}$$

where $S_{sat}(-\Delta\omega)$ is the measured water signal with RF saturation at frequency offset $-\Delta\omega$, $S_{sat}(\Delta\omega)$ with RF saturation at $\Delta\omega$ and S_0 without RF saturation. This means that to calculate MTR_{asym}, measurements at both $\Delta\omega$ and $-\Delta\omega$ are needed, assuming MTC and direct water saturation effects are symmetric and that the magnetic field (and therefore water frequency) is both uniform and constant. This assumption is true only to some extent, which will be discussed further. MTR consists of a mix of signal contributions, that is, from MT, CEST, and the direct effect, but it has higher signal-to-noise ratio compared to MTR_{asym} because MTR_{asym} propagates the error from two S_{sat} measurements. MTR can be a useful parameter in addition to more quantitative parameters that attempt to eliminate the T1 effects. For example, MTR maps have been shown to provide differentiation between tumor progression and radiation necrosis in brain metastasis patients.[15,16]

To describe and analyze the frequency offset-dependent saturation effects in CEST, an understanding of two commonly used plots is essential (Figure 2). The first plot is the CEST Z-spectrum. The horizontal axis is the frequency offset with the resonance of water at 0 ppm and the vertical axis is the ratio of water signal with saturation (S_{sat}) to water signal without saturation (S_0) at each given frequency offset. The CEST effects can be seen at the specific saturation frequency offsets of interest. As expected, the lowest point of the curve is at 0 ppm due to the direct saturation of water. The second plot (lower left corners in Figure 2) is the MTR asymmetry spectrum, where the signal at the opposite frequency offset has been subtracted to remove the effects of MTC and direct water saturation. However, a typical CEST experiment would collect images at only a few offsets, rather than measuring the entire Z-spectrum.

Another technique that has been used to remove some of the direct effect of water saturation is called Lorentzian difference (LD) analysis. This technique fits a Lorentzian function to the points on a Z-spectrum with minimal CEST effects to estimate the direct effect at all frequency offsets. Measurements typically fitted include those at high ($|\Delta\omega| > 10$ ppm[17] or ≥ 6 ppm[18,19]) and low ($|\Delta\omega| < 1.75$ ppm[19] or < 1 ppm[17,18]) frequency offsets. Then, the measured Z-spectrum values at the amide CEST frequency offset and its opposite (3.5 and -3.5 ppm, respectively) are subtracted from the Lorentzian values interpolated to those offsets to produce the LD signal. Furthermore, the measurements used to fit the Lorentzian likely have contributions from MTC unless the saturation amplitude is very low and therefore the fitted Lorentzian will only be an approximation of the signal from the direct effect.
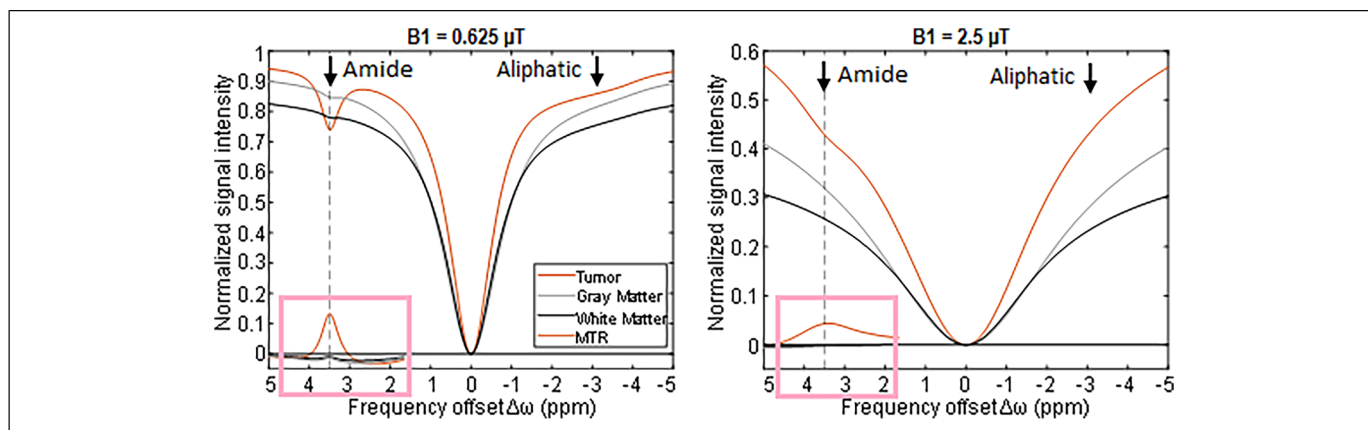
Figure 2. Simulated Z-spectra, with 2 different radiofrequency pulse amplitudes (B1) of 0.625 and 2.5 µT at 3T. The water resonance is defined to be 0 ppm. The amide (CEST) peak and center of the broad aliphatic (rNOE) peak are indicated. MTR asymmetry curve is shown in the left lower corner of each Z-spectra plot.
Abbreviations: CEST, chemical exchange saturation transfer; rNOE, relayed nuclear Overhauser effect; MTR, magnetization transfer ratio.

Factors Affecting the CEST Signal

In order to accurately measure the CEST signal, the following need to be considered:

(a). **Magnetic field (B0) inhomogeneities:** CEST measurements are performed at one or more frequency offset(s). This assumes that the resonance frequency of water is at 0 ppm in each voxel. However, B0 inhomogeneities related to hardware and susceptibility changes related to patient anatomy (eg, near paranasal sinuses) create a shift in the B0 field, altering the actual frequency offset being saturated. This results in an apparent shift in the Z-spectrum along the *x*-axis (Figure 3). A commonly used correction technique densely and symmetrically samples spectral frequency at different offsets around the reference frequency. Techniques such as water saturation shift referencing (WASSR)[20] or simultaneous mapping of water shift and B1 (WASABI)[21] can then shift the Z-spectrum during postprocessing to recenter the water peak with the lowest point back to 0 ppm. Note that WASSR and WASABI scans should be performed separately from the CEST sequences. Alternatively, a much quicker way is to separately acquire a ΔB0 map to directly shift the Z-spectrum by the voxelwise ΔB0 value.[22]

(b). **RF field (B1) inhomogeneities:** The magnitude of the CEST effect is dependent on the saturation pulse(s) and, thus, an accurate amplitude B1 is required for quantification and reproducibility. However, RF inhomogeneity can cause variability in the amplitude of the RF pulse, resulting in an actual B1 amplitude that is different from the prescribed B1 amplitude. This can cause the CEST effect to be spatially inhomogeneous even in phantoms that have a known and uniform CEST effect.[23] Furthermore, errors related to B1

inhomogeneities appear as a change in the shape of the Z-spectrum (Figure 3) and are generally nonlinear with respect to the frequency offset as well as applied B1 amplitude. These errors can be corrected in the same way as B0 inhomogeneities—by acquiring a B1 map and CEST data at several closely-spaced RF powers—however, these errors are more difficult to correct and require additional data such as B1 calibration maps, dual-transmit RF systems and more sophisticated data processing or model fitting using CEST scans collected with multiple nominal B1 amplitudes.[24]

(c). **Relayed nuclear Overhauser effect (rNOE):** The rNOE effect has been attributed to aliphatic and olefinic protons[17,25] in mobile macromolecules and is of unique importance,[26,27] where it has been shown to decrease in tumors compared to healthy brain tissue.[17,28] Effects from these chemical groups are evident as a broad peak in the Z-spectrum in the range of ≈ −1 to −4 ppm. rNOE is a multistep process. The first step is the saturation of a proton on the mobile macromolecule. The second step is through-space cross relaxation where the saturated magnetization is swapped with nonsaturated magnetization in an adjacent proton, such as on a hydroxyl group that is covalently bonded, or a water molecule that is hydrogen bound to the mobile macromolecule. Note that protons do not physically switch places as occurs in CEST. The third step is for the proton on the hydroxyl group to undergo CEST or the bound water molecule to be replaced with a free water molecule.[29] The rNOE proton exchange rate is estimated to be around 16 Hz and the T2 to be at least an order of magnitude lower than that of the non-rNOE CEST exchange.[10,13] The use of the rNOE-CEST effect for imaging is of unique importance, as exemplified by findings in glioma patients.[30–32] Clinical application
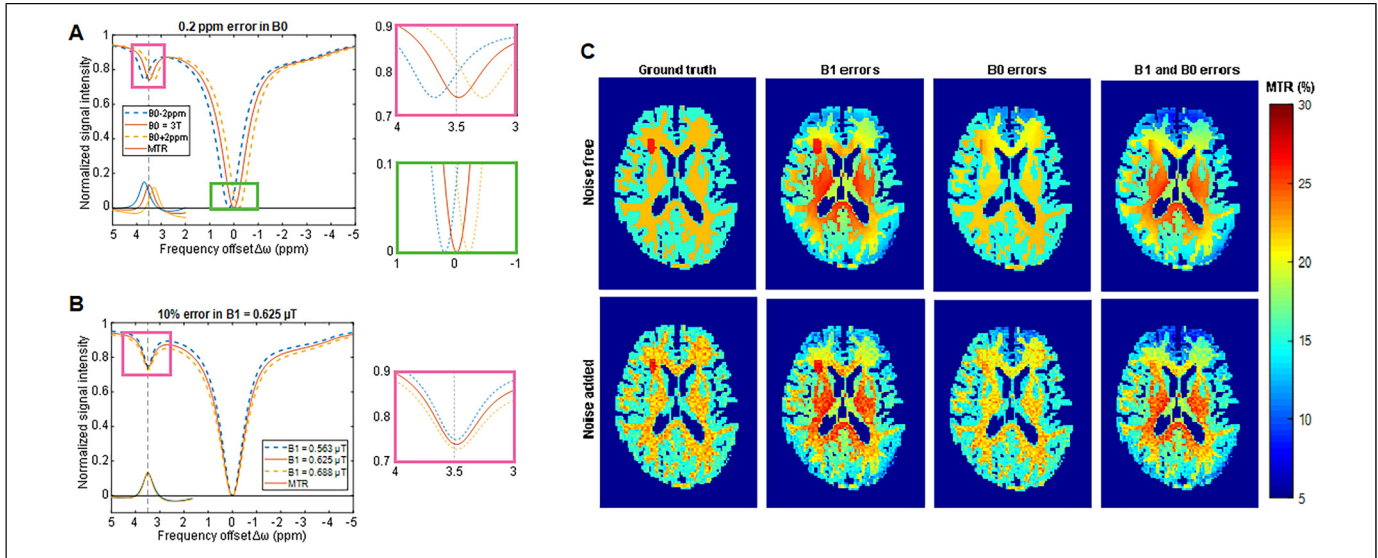
Figure 3. (A) Effect of B0 error as a shift to left (blue dotted line) or shift to right (orange dotted line) in the Z-spectrum and resultant underestimation of the APT signal. The solid red curve shows the corrected simulated spectrum. (B) Effect of B1 errors as a change in shape of the Z-spectrum. The corrected simulated spectrum is shown in red, the dotted curves demonstrate the effect of B1 errors, either 10% lower (blue) or 10% higher (orange) than prescribed, for a B1 of 0.625 μT. (C) Simulated MTR amide images of the brain at 3T (B1 = 0.625 μT) with gray and white matter, and a small simulated tumor in the right frontal region, showing the ground truth (left column), the effects of B1 and B0 errors both individually (middle columns), and combined (right column), in a noise-free simulation (top row) and a simulation with noise added (bottom row).
Abbreviations: MTR, magnetization transfer ratio; APT, amide proton transfer.

of CEST can be performed with the investigation of both APT and rNOE effects, especially as the NOE signal will affect the APT imaging. The presence of rNOE complicates CEST measurements, as the background signal is no longer symmetric. At high B1 power (> 2 μT), the contribution of magnetization transfer contrast (MTC) to the saturated CEST signal becomes greater than the effects of APT and NOE. However, the NOE effect cannot completely be eliminated.[13,33,34] rNOE is itself an emerging MR biomarker in neuro-oncology.

Practical Considerations

a. Effect of field strength: Increased field strength is advantageous to CEST as there is increased separation of signals, since the frequencies involved are much larger, and increased signal to noise ratio due to greater polarization. Another advantage is that a higher field strength leads to longer T1 relaxation time without affecting exchange rate, which increases the fraction of saturated protons and thus increasing CEST signal. Although CEST imaging is best at field strengths of 3T or higher, there have been CEST imaging performed at lower field strengths. This includes applications in glioma on 1.5T conventional scanner[35] as well as the 1.5T MR-Linac, a hybrid MRI and radiation treatment device.[36]

b. Contrast agents: Although exogenous contrast agents have been used for CEST studies, most human CEST experiments have investigated signal from endogenous molecules with exchangeable protons in amide (3.5 ppm), amine (3 ppm), guanidinium (2 ppm), and hydroxyl groups (0.5-1.5 ppm).[10,13] The most commonly studied CEST technique, APT, is focused on amide protons where the major source of amide is from dissolved proteins and peptides.[37,38] Tumoral tissues can have increased concentration of proteins and peptides compared to normal brain making them an ideal candidate for APT imaging. As the CEST effect is dependent on T1 effects, CEST imaging should be performed before the administration of any contrast agent, including for example, gadolinium-based agents that reduce T1 relaxation time.

c. Acquisition time: Like any MRI acquisition, optimal CEST imaging is an interplay between acquisition time, image contrast and noise. In the past, most CEST experiments were limited to single-slice acquisitions, reducing its clinical applicability. Recently, significant efforts have been made to accelerate CEST imaging using both acquisition- and reconstruction-oriented approaches,[39] enabling whole brain imaging with reasonable scan times. For example, a 3D APT protocol,[3] where APT CEST are performed using 7 frequency offsets (at ±3.1, ±3.5, ±3.9 ppm with a reference scan) with concatenated RF pulses from 2 amplifiers and dixon-based ΔB0 mapping, is now able to produce a 10-slice volumetric image in 4 min and 8 s, with a resolution of $1.8 \times 1.8 \times 6$ mm.[3]

Long continuous RF pulses (∼5 s) are ideal for CEST but are not practical in clinical settings due to hardware, and more importantly SAR limitations. Various saturation pulses have been designed to improve the sensitivity and efficiency of CEST including pulse-train,[3] pulsed steady-state,[40] and unevenly segmented RF saturation.[41] In addition, several innovative saturation editing sequences have been proposed.[42–46] Fast readout sequences improve readout efficiency and decrease scan time. Turbo spin-echo is the most common readout approach used for CEST imaging on clinical scanners,[47] as it does not suffer from susceptibility-related distortion and ghosting from lipids as seen with echo-planar-based sequences.[48] Other readout sequences or alternative saturation approaches including ultrafast Z-spectroscopy[49] can also be used to accelerate the acquisition.[34,50] Parallel imaging,[51] compressed sensing,[52,53] or combination of both[54] and keyhole imaging[55] can also be used to speed-up acquisition. Other promising techniques include magnetic resonance fingerprinting[56] and nonFourier transform-based techniques based on manifold learning.[57]

d. **Measurement reliability:** Reproducibility between vendors and sites is very important for clinical applicability of CEST, as it enables results from different cohorts to be compared.[58–60] Generally, there is no standardization for CEST postprocessing. However, recent consensus recommendations have been published to address this issue.[3] Studies have shown good repeatability in healthy subjects.[60,61] In patients, repeatability is region-dependent, with better repeatability in supratentorial lesions compared to infratentorial lesions due to B0 inhomogeneity and susceptibility effects.[62] In recent work,[63]
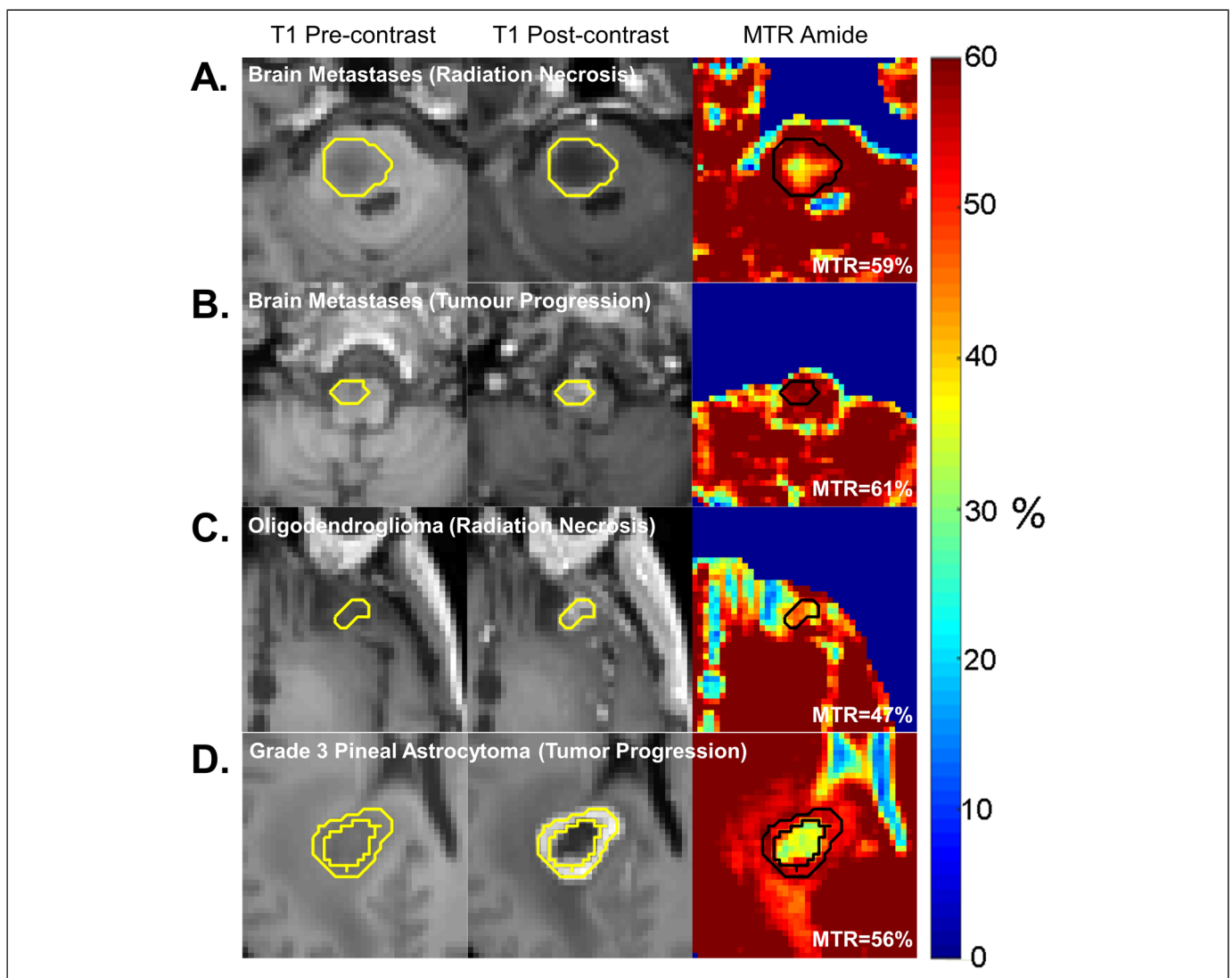

Figure 4. Chemical exchange saturation transfer (CEST) for differentiation of tumor progression versus radiation necrosis: examples of radiation necrosis (A) and tumor progression (B) are shown for patients with brain metastases following stereotactic radiosurgery. Examples of glioma are shown following chemoradiation, including an oligodendroglioma with radiation necrosis (C) and a progressed grade 3 astrocytoma (D). All images are of selected slices from the 3D CEST acquisition at 3T.
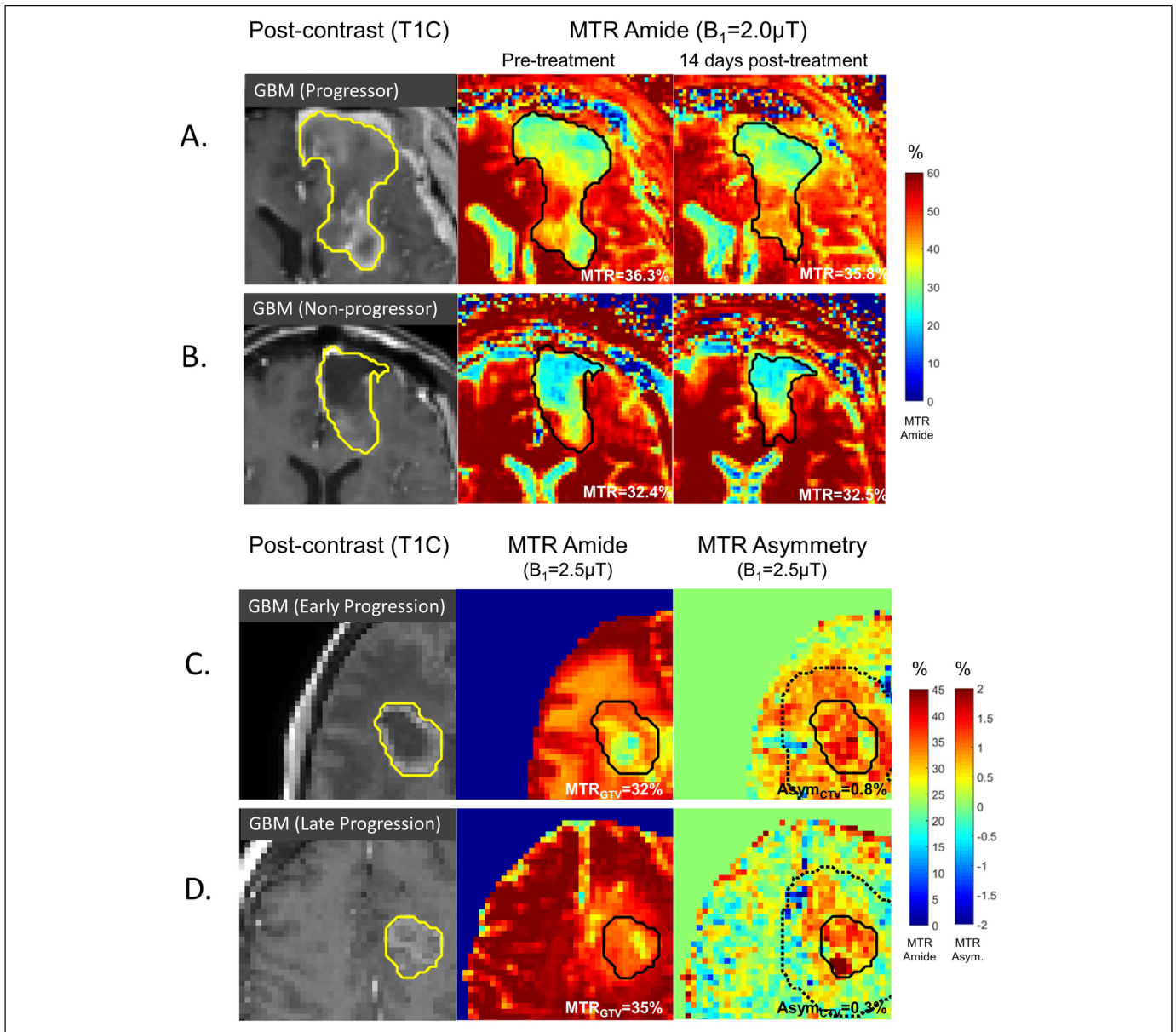
Figure 5. CEST for predicting treatment response in glioblastoma: (A, B) MTR amide maps from single-slice CEST at 3T are shown before treatment at the time of radiation planning MRI (middle column) and at 14 days after the start of radiation (right column) for patients demonstrating early progression in (A) versus late progression in (B). (C, D) Images at the time of radiation planning MRI are shown of the MTR amide map (middle column) and the MTR asymmetry map (right column). The solid lines include the enhancing tumor plus the resection cavity. The dotted lines on the MTR asymmetry maps represent the clinical target volume. Regions of high MTR asymmetry in the CTV were associated with early progression (C). An example of late progression (D) is also shown.

Abbreviations: CEST, chemical exchange saturation transfer; MTR, magnetization transfer ratio; MRI, magnetic resonance imaging; CTV, clinical target volume.

cross-vendor comparisons showed improved correspondence when the CEST signal was scaled by the contralateral normal-appearing white matter signal.

Emerging Clinical Applications

Differentiating Tumor Progression From Treatment Response

CEST, in particular APT CEST, can be added to the existing armamentarium of structural and physiologic imaging such as diffusion weighted imaging (DWI), perfusion weighted imaging (PWI), and MRS. In particular, CEST has particular applicability in differentiating between tumor progression and treatment response in metastatic brain disease treated with radiation, or in gliomas treated with chemoradiation. Tumor progression results in higher concentration of proteins and peptides with amide groups, resulting in higher signal compared to radiation necrosis, where cellular derived protein concentrations are low (Figure 4).[64] Several studies have demonstrated that the addition of CEST to PWI and DWI metrics increases

the diagnostic accuracy in differentiating tumor progression from treatment effects in patients with glioblastoma (AUC, 0.95-0.97 vs 0.84-0.91[65] and AUC, 0.87 vs 0.92[66]). Studies to assess the additional benefit of CEST in the setting of metastatic brain disease are ongoing with a recent study showing CEST metrics were shown to differentiate radiation necrosis from tumor progression a group of 70 patients (75 lesions) with metastatic brain disease (AUC up to 0.88).[15]

Evaluation of Treatment Response

Studies conducted at 1.5 and 3T have demonstrated the potential to predict response to therapy in glioblastoma. Changes in MTR values between radiation planning MRI and 14 days following start of chemoradiation can identify patients who demonstrate early progression[67] (Figure 5). High MTR values in the clinical target volume (CTV), defined as enhancing tumor and resection cavity with 2 to 3 cm margin which receives the highest radiation dose, before the start of chemoradiation are associated with early progression[36] (Figure 5). In agreement with the known relationship between acidity and glioblastoma, a study of 20 patients with glioblastoma using amine CEST to determine pH demonstrated that patients with low acidity tumors have longer progression free survival compared to those with tumors showing stable or increased acidity postoperatively or throughout follow-up.[68] Compared to glioblastoma, literature regarding CEST in brain metastasis is limited. In a group of 25 patients with brain metastasis undergoing stereotactic radiosurgery, CEST metrics in contralateral WM were strongly correlated with volume change of metastatic lesions at 1-month postradiation.[69]

Other Applications

Clinical CEST applications include those that measure the APT effect for improved diagnosis of brain tumors, for example, in distinguishing brain metastases from glioblastoma,[71] and also in differentiating lymphomas from high-grade gliomas,[72] partially achieved by comparing the APT signal in areas of peritumoral edema. As well, CEST has been investigated to predict grading of the gliomas demonstrating higher APT signal in high versus low-grade glioma.[70] However, most of the research studies in this area have been conducted before the release of new WHO classification of brain tumors which includes an array of new molecular and cytogenetic markers for tumor classification as opposed to purely microscopic features that were available at the time of these studies.[73] CEST has been investigated to determine the molecular subtype of gliomas. Increased CEST effect in gliomas is observed with wild-type isocitrate dehydrogenase (IDH) gliomas compared to those with mutant IDH.[30,74] Likewise, increased signal is observed in glioblastomas with unmethylated O6-methylguanine-DNA methyltransferase (MGMT) compared to their methylated counterparts.[75] In addition, a positive correlation between CEST signal and tumor proliferation index (Ki-67 labeling) has been shown.[76] Research in this area is still ongoing in light of new molecular

biomarkers and technology.[73] Besides APT CEST, amine CEST and GlucoCEST are examples of other applications that have also been explored in neuro-oncology.[77,78]

Conclusion

In this article, basic principles of CEST were summarized for clinicians in neuro-oncological practice and several important areas were addressed where CEST MRI could provide added value to clinical care. This is an evolving field with many technical developments underway. For more detail, readers are encouraged to consult more in-depth publications[3,7,79,80] and the references therein.

ORCID iDs

Pejman Jabehdar Maralani https://orcid.org/0000-0001-9975-4379
Ryan Oglesby https://orcid.org/0000-0002-6972-8214

References

1. Forsén S, Hoffman RA. Study of moderately rapid chemical exchange reactions by means of nuclear magnetic double resonance. *J Chem Phys.* 1963;39(11):2892-2901. doi:10.1063/1.1734121
2. Ward KM, Aletras AH, Balaban RS. A new class of contrast agents for MRI based on proton chemical exchange dependent

saturation transfer (CEST). *J Magn Reson.* 2000;143(1):79-87. doi:10.1006/jmre.1999.1956

3. Zhou J, Zaiss M, Knutsson L, et al. Review and consensus recommendations on clinical APT-weighted imaging approaches at 3T: application to brain tumors. *Magn Reson Med.* 2022;88(2):546-574. doi:10.1002/mrm.29241

4. Farrar CT, Buhrman JS, Liu G,. et al. Establishing the lysine-rich protein CEST reporter gene as a CEST MR imaging detector for oncolytic virotherapy. *Radiology.* 2015;275(3):746-754. doi:10.1148/radiol.14140251

5. Ren J, Trokowski R, Zhang S, Malloy CR, Sherry AD. Imaging the tissue distribution of glucose in livers using a PARACEST sensor. *Magn Reson Med.* 2008;60(5):1047-1055. doi:10.1002/mrm.21722

6. Hampton DG, Goldman-Yassen AE, Sun PZ, Hu R. Metabolic magnetic resonance imaging in neuroimaging: magnetic resonance spectroscopy, sodium magnetic resonance imaging and chemical exchange saturation transfer. *Semin Ultrasound CT MRI.* 2021;42(5):452-462. doi:10.1053/j.sult.2021.07.003

7. van Zijl PCM, Yadav NN. Chemical exchange saturation transfer (CEST): What is in a name and what isn't? *Magn Reson Med.* 2011;65(4):927-948. doi:10.1002/mrm.22761

8. Wada T, Togao O, Tokunaga C, Funatsu R, Kobayashi K, Nakamura Y. Effect of the saturation pulse duration on chemical exchange saturation transfer in amide proton transfer MR imaging: a phantom study. *Radiol Phys Technol.* 2016;9(1):15-21. doi:10.1007/s12194-015-0326-1

9. Tokunaga C, Wada T, Togao O, Yamashita Y, Kobayashi K, Kato T. Effect of saturation pulse duration and power on pH-weighted amide proton transfer imaging: a phantom study. *Magn Reson Med Sci.* 2022; 22(4): 487-495. doi:10.2463/mrms.mp.2021-0109

10. Zaiss M, Jin T, Kim S, Gochberg DF. Theory of chemical exchange saturation transfer MRI in the context of different magnetic fields. *NMR Biomed.* 2022;35(11):e4789. doi:10.1002/nbm.4789

11. Zaiß M, Schmitt B, Bachert P. Quantitative separation of CEST effect from magnetization transfer and spillover effects by Lorentzian-line-fit analysis of z-spectra. *J Magn Reson.* 2011;211(2):149-155. doi:10.1016/j.jmr.2011.05.001

12. Kucharczyk W, Macdonald PM, Stanisz GJ, Henkelman RM. Relaxivity and magnetization transfer of white matter lipids at MR imaging: importance of cerebrosides and pH. *Radiology.* 1994;192(2):521-529. doi:10.1148/radiology.192.2.8029426

13. van Zijl PCM, Lam WW, Xu J, Knutsson L, Stanisz GJ. Magnetization transfer contrast and chemical exchange saturation transfer MRI. Features and analysis of the field-dependent saturation spectrum. *NeuroImage.* 2018;168:222-241. doi:10.1016/j.neuroimage.2017.04.045

14. Stanisz GJ, Odrobina EE, Pun J, et al. T_1, T_2 relaxation and magnetization transfer in tissue at 3T. *Magn Reson Med.* 2005;54(3):507-512. doi:10.1002/mrm.20605

15. Mehrabian H, Chan RW, Sahgal A, et al. Chemical exchange saturation transfer MRI for differentiating radiation necrosis from tumor progression in brain metastasis—application in a clinical setting. *J Magn Reson Imaging.* 2023;57(6):1713-1725. doi:10.1002/jmri.28440

16. Mehrabian H, Desmond KL, Soliman H, Sahgal A, Stanisz GJ. Differentiation between radiation necrosis and tumor progression using chemical exchange saturation transfer. *Clin Cancer Res.* 2017;23(14):3667-3675. doi:10.1158/1078-0432.CCR-16-2265

17. Jones CK, Huang A, Xu J, et al. Nuclear Overhauser enhancement (NOE) imaging in the human brain at 7T. *NeuroImage.* 2013;77:114-124. doi:10.1016/j.neuroimage.2013.03.047

18. Jones CK, Polders D, Hua J, et al. In vivo three-dimensional whole-brain pulsed steady-state chemical exchange saturation transfer at 7T. *Magn Reson Med.* 2012;67(6):1579-1589. doi:10.1002/mrm.23141

19. Warnert EAH, Wood TC, Incekara F, et al. Mapping tumour heterogeneity with pulsed 3D CEST MRI in non-enhancing glioma at 3T. *Magn Reson Mater Phys Biol Med.* 2022;35(1):53-62. doi:10.1007/s10334-021-00911-6

20. Kim M, Gillen J, Landman BA, Zhou J, van Zijl PCM. Water saturation shift referencing (WASSR) for chemical exchange saturation transfer (CEST) experiments. *Magn Reson Med.* 2009;61(6):1441-1450. doi:10.1002/mrm.21873

21. Schuenke P, Windschuh J, Roeloffs V, Ladd ME, Bachert P, Zaiss M. Simultaneous mapping of water shift and B_1 (WASABI)—application to field-inhomogeneity correction of CEST MRI data. *Magn Reson Med.* 2017;77(2):571-580. doi:10.1002/mrm.26133

22. Togao O, Keupp J, Hiwatashi A, et al. Amide proton transfer imaging of brain tumors using a self-corrected 3D fast spin-echo dixon method: comparison with separate B_0 correction. *Magn Reson Med.* 2017;77(6):2272-2279. doi:10.1002/mrm.26322

23. Singh A, Cai K, Haris M, Hariharan H, Reddy R. On B_1 inhomogeneity correction of in vivo human brain glutamate chemical exchange saturation transfer contrast at 7T. *Magn Reson Med.* 2013;69(3):818-824. doi:10.1002/mrm.24290

24. Liu G, Song X, Chan KWY, McMahon MT. Nuts and bolts of chemical exchange saturation transfer MRI. *NMR Biomed.* 2013;26(7):810-828. doi:10.1002/nbm.2899

25. Heo HY, Zhang Y, Lee DH, Hong X, Zhou J. Quantitative assessment of amide proton transfer (APT) and nuclear Overhauser enhancement (NOE) imaging with extrapolated semi-solid magnetization transfer reference (EMR) signals: application to a rat glioma model at 4.7 tesla. *Magn Reson Med.* 2016;75(1):137-149. doi:10.1002/mrm.25581

26. Zhou J, Hong X, Zhao X, Gao JH, Yuan J. APT-weighted and NOE-weighted image contrasts in glioma with different RF saturation powers based on magnetization transfer ratio asymmetry analyses. *Magn Reson Med.* 2013;70(2):320-327. doi:10.1002/mrm.24784

27. Zaiss M, Windschuh J, Paech D, et al. Relaxation-compensated CEST-MRI of the human brain at 7T: unbiased insight into NOE and amide signal changes in human glioblastoma. *NeuroImage.* 2015;112:180-188. doi:10.1016/j.neuroimage.2015.02.040

28. Zaiss M, Bachert P. Chemical exchange saturation transfer (CEST) and MR Z-spectroscopy in vivo: a review of theoretical approaches and methods. *Phys Med Biol.* 2013;58(22):R221-R269. doi:10.1088/0031-9155/58/22/R221

29. Zhou Y, Bie C, van Zijl PCM, Yadav NN. The relayed nuclear Overhauser effect in magnetization transfer and chemical

exchange saturation transfer MRI. *NMR Biomed.* 2023;36(6): e4778. doi:10.1002/nbm.4778

30. Paech D, Windschuh J, Oberhollenzer J, et al. Assessing the predictability of IDH mutation and MGMT methylation status in glioma patients using relaxation-compensated multipool CEST MRI at 7.0T. *Neuro-Oncol.* 2018;20(12):1661-1671. doi:10.1093/neuonc/noy073

31. Regnery S, Adeberg S, Dreher C, et al. Chemical exchange saturation transfer MRI serves as predictor of early progression in glioblastoma patients. *Oncotarget.* 2018;9(47):28772-28783. doi:10.18632/oncotarget.25594

32. Heo HY, Jones CK, Hua J, et al. Whole-brain amide proton transfer (APT) and nuclear overhauser enhancement (NOE) imaging in glioma patients using low-power steady-state pulsed chemical exchange saturation transfer (CEST) imaging at 7T. *J Magn Reson Imaging.* 2016;44(1):41-50. doi:10.1002/jmri.25108

33. Wu Y, Wood TC, Arzanforoosh F, et al. 3D APT and NOE CEST-MRI of healthy volunteers and patients with non-enhancing glioma at 3T. *Magn Reson Mater Phys Biol Med.* 2022;35(1):63-73. doi:10.1007/s10334-021-00996-z

34. Deshmane A, Zaiss M, Lindig T, et al. 3D gradient echo snapshot CEST MRI with low power saturation for human studies at 3T. *Magn Reson Med.* 2019;81(4):2412-2423. doi:10.1002/mrm.27569

35. Chan RW, Myrehaug S, Stanisz GJ, Sahgal A, Lau AZ. Quantification of pulsed saturation transfer at 1.5T and 3T. *Magn Reson Med.* 2019;82(5):1684-1699. doi:10.1002/mrm.27856

36. Chan RW, Lawrence LSP, Oglesby RT, et al. Chemical exchange saturation transfer MRI in central nervous system tumours on a 1.5T MR-linac. *Radiother Oncol.* 2021;162:140-149. doi:10.1016/j.radonc.2021.07.010

37. Zhou J, Payen JF, Wilson DA, Traystman RJ, van Zijl PCM. Using the amide proton signals of intracellular proteins and peptides to detect pH effects in MRI. *Nat Med.* 2003;9(8):1085-1090. doi:10.1038/nm907

38. Zhou J, Tryggestad E, Wen Z, et al. Differentiation between glioma and radiation necrosis using molecular magnetic resonance imaging of endogenous proteins and peptides. *Nat Med.* 2011;17(1):130-134. doi:10.1038/nm.2268

39. Zhang Y, Zu T, Liu R, Zhou J. Acquisition sequences and reconstruction methods for fast chemical exchange saturation transfer imaging. *NMR Biomed.* 2023;36(6):e4699. doi:10.1002/nbm.4699

40. Khlebnikov V, Geades N, Klomp DWJ, Hoogduin H, Gowland P, Mougin O. Comparison of pulsed three-dimensional CEST acquisition schemes at 7 tesla: steady state versus pseudosteady state. *Magn Reson Med.* 2017;77(6):2280-2287. doi:10.1002/mrm.26323

41. Sun PZ, Cheung JS, Wang E, Benner T, Sorensen AG. Fast multi-slice pH-weighted chemical exchange saturation transfer (CEST) MRI with unevenly segmented RF irradiation. *Magn Reson Med.* 2011;65(2):588-594. doi:10.1002/mrm.22628

42. Scheidegger R, Vinogradov E, Alsop DC. Amide proton transfer imaging with improved robustness to magnetic field inhomogeneity and magnetization transfer asymmetry using saturation with

frequency alternating RF irradiation. *Magn Reson Med.* 2011;66(5):1275-1285. doi:10.1002/mrm.22912

43. Song X, Gilad AA, Joel S, et al. CEST phase mapping using a length and offset varied saturation (LOVARS) scheme. *Magn Reson Med.* 2012;68(4):1074-1086. doi:10.1002/mrm.23312

44. Zu Z, Janve VA, Xu J, Does MD, Gore JC, Gochberg DF. A new method for detecting exchanging amide protons using chemical exchange rotation transfer. *Magn Reson Med.* 2013;69(3):637-647. doi:10.1002/mrm.24284

45. Xu J, Yadav NN, Bar-Shir A, et al. Variable delay multi-pulse train for fast chemical exchange saturation transfer and relayed-nuclear Overhauser enhancement MRI. *Magn Reson Med.* 2014;71(5):1798-1812. doi:10.1002/mrm.24850

46. Friedman JI, McMahon MT, Stivers JT, Van Zijl PCM. Indirect detection of labile solute proton spectra via the water signal using frequency-labeled exchange (FLEX) transfer. *J Am Chem Soc.* 2010;132(6):1813-1815. doi:10.1021/ja909001q

47. Zhao X, Wen Z, Zhang G, et al. Three-dimensional turbo-spin-echo amide proton transfer MR imaging at 3-tesla and its application to high-grade human brain tumors. *Mol Imaging Biol.* 2013;15(1):114-122. doi:10.1007/s11307-012-0563-1

48. Sun PZ, Zhou J, Sun W, Huang J, van Zijl PCM. Suppression of lipid artifacts in amide proton transfer imaging. *Magn Reson Med.* 2005;54(1):222-225. doi:10.1002/mrm.20530

49. Xu X, Lee JS, Jerschow A. Ultrafast scanning of exchangeable sites by NMR spectroscopy. *Angew Chem Int Ed.* 2013;52(32):8281-8284. doi:10.1002/anie.201303255

50. Zaiss M, Ehses P, Scheffler K. Snapshot-CEST: optimizing spiral-centric-reordered gradient echo acquisition for fast and robust 3D CEST MRI at 9.4T. *NMR Biomed.* 2018;31(4):e3879. doi:10.1002/nbm.3879

51. Zhang Y, Heo HY, Lee DH, et al. Chemical exchange saturation transfer (CEST) imaging with fast variably-accelerated sensitivity encoding (vSENSE). *Magn Reson Med.* 2017;77(6):2225-2238. doi:10.1002/mrm.26307

52. Lustig M, Donoho D, Pauly JM. Sparse MRI: the application of compressed sensing for rapid MR imaging. *Magn Reson Med.* 2007;58(6):1182-1195. doi:10.1002/mrm.21391

53. Wada T, Tokunaga C, Togao O, et al. Three-dimensional chemical exchange saturation transfer imaging using compressed SENSE for full z-spectrum acquisition. *Magn Reson Imaging.* 2022;92:58-66. doi:10.1016/j.mri.2022.05.014

54. She H, Greer JS, Zhang S, et al. Accelerating chemical exchange saturation transfer MRI with parallel blind compressed sensing. *Magn Reson Med.* 2019;81(1):504-513. doi:10.1002/mrm.27400

55. Varma G, Lenkinski RE, Vinogradov E. Keyhole chemical exchange saturation transfer. *Magn Reson Med.* 2012;68(4):1228-1233. doi:10.1002/mrm.23310

56. Zhou Z, Han P, Zhou B, et al. Chemical exchange saturation transfer fingerprinting for exchange rate quantification. *Magn Reson Med.* 2018;80(4):1352-1363. doi:10.1002/mrm.27363

57. Zhu B, Liu JZ, Cauley SF, Rosen BR, Rosen MS. Image reconstruction by domain-transform manifold learning. *Nature.* 2018;555(7697):487-492. doi:10.1038/nature25988

58. Togao O, Hiwatashi A, Keupp J, et al. Scan–rescan reproducibility of parallel transmission based amide proton transfer imaging of brain tumors. *J Magn Reson Imaging.* 2015;42(5):1346-1353. doi:10.1002/jmri.24895

59. Wamelink IJHG, Kuijer JPA, Padrela BE, et al. Reproducibility of 3 T APT-CEST in healthy volunteers and patients with brain glioma. *J Magn Reson Imaging.* 2023;57(1):206-215. doi:10.1002/jmri.28239

60. Voelker MN, Kraff O, Goerke S, et al. The traveling heads 2.0: multicenter reproducibility of quantitative imaging methods at 7 Tesla. *NeuroImage.* 2021;232(January):117910. doi:10.1016/j.neuroimage.2021.117910

61. Leutritz T, Seif M, Helms G, et al. Multiparameter mapping of relaxation (R1, R2*), proton density and magnetization transfer saturation at 3T: A multicenter dual-vendor reproducibility and repeatability study. *Hum Brain Mapp.* 2020;41(15):4232-4247. doi:10.1002/hbm.25122

62. Lee JB, Park JE, Jung SC, et al. Repeatability of amide proton transfer-weighted signals in the brain according to clinical condition and anatomical location. *Eur Radiol.* 2020;30(1):346-356. doi:10.1007/s00330-019-06285-7

63. Chan RW, Lam WW, Liebig P, et al. Differentiating radiation necrosis from tumour progression in brain metastases using CEST: a cross-vendor comparison. In: *Proceedings of the Joint Annual Meeting of ISMRM-ESMRMB*; 2022:4458.

64. Wu B, Warnock G, Zaiss M, et al. An overview of CEST MRI for non-MR physicists. *EJNMMI Phys.* 2016;3(1):19. doi:10.1186/s40658-016-0155-2

65. Park KJ, Kim HS, Park JE, Shim WH, Kim SJ, Smith SA. Added value of amide proton transfer imaging to conventional and perfusion MR imaging for evaluating the treatment response of newly diagnosed glioblastoma. *Eur Radiol.* 2016;26(12):4390-4403. doi:10.1007/s00330-016-4261-2

66. Park YW, Ahn SS, Kim EH, et al. Differentiation of recurrent diffuse glioma from treatment-induced change using amide proton transfer imaging: incremental value to diffusion and perfusion parameters. *Neuroradiology.* 2021;63(3):363-372. doi:10.1007/s00234-020-02542-5

67. Mehrabian H, Myrehaug S, Soliman H, Sahgal A, Stanisz GJ. Evaluation of glioblastoma response to therapy with chemical exchange saturation transfer. *Int J Radiat Oncol.* 2018;101(3):713-723. doi:10.1016/j.ijrobp.2018.03.057

68. Harris RJ, Cloughesy TF, Liau LM, et al. pH-weighted molecular imaging of gliomas using amine chemical exchange saturation transfer MRI. *Neuro-Oncol.* 2015;17(11):1514-1524. doi:10.1093/neuonc/nov106

69. Desmond KL, Mehrabian H, Chavez S, et al. Chemical exchange saturation transfer for predicting response to stereotactic radiosurgery in human brain metastasis. *Magn Reson Med.* 2017;78(3):1110-1120. doi:10.1002/mrm.26470

70. Sotirios B, Demetriou E, Topriceanu CC, Zakrzewska Z. The role of APT imaging in gliomas grading: a systematic review and meta-analysis. *Eur J Radiol.* 2020;133:109353. doi:10.1016/j.ejrad.2020.109353

71. Yu H, Lou H, Zou T, et al. Applying protein-based amide proton transfer MR imaging to distinguish solitary brain metastases from glioblastoma. *Eur Radiol.* 2017;27(11):4516-4524. doi:10.1007/s00330-017-4867-z

72. Jiang S, Yu H, Wang X, et al. Molecular MRI differentiation between primary central nervous system lymphomas and high-grade gliomas using endogenous protein-based amide proton transfer MR imaging at 3 tesla. *Eur Radiol.* 2016;26(1):64-71. doi:10.1007/s00330-015-3805-1

73. Louis DN, Perry A, Wesseling P, et al. The 2021 WHO classification of tumors of the central nervous system: a summary. *Neuro-Oncol.* 2021;23(8):1231-1251. doi:10.1093/neuonc/noab106

74. Sakata A, Okada T, Yamamoto A, et al. Grading glial tumors with amide proton transfer MR imaging: different analytical approaches. *J Neurooncol.* 2015;122(2):339-348. doi:10.1007/s11060-014-1715-8

75. Paech D, Zaiss M, Meissner JE, et al. Nuclear overhauser enhancement mediated chemical exchange saturation transfer imaging at 7 tesla in glioblastoma patients. Herholz K, ed. *PLoS ONE.* 2014;9(8):e104181. doi:10.1371/journal.pone.0104181

76. Zhang J, Zhu W, Tain R, Zhou XJ, Cai K. Improved differentiation of low-grade and high-grade gliomas and detection of tumor proliferation using APT contrast fitted from Z-spectrum. *Mol Imaging Biol.* 2018;20(4):623-631. doi:10.1007/s11307-017-1154-y

77. Cho NS, Hagiwara A, Yao J, et al. Amine-weighted chemical exchange saturation transfer magnetic resonance imaging in brain tumors. *NMR Biomed.* 2023;36(6):e4785. doi:10.1002/nbm.4785

78. Bender B, Herz K, Deshmane A, et al. GLINT: GlucoCEST in neoplastic tumors at 3T—clinical results of GlucoCEST in gliomas. *Magn Reson Mater Phys Biol Med.* 2022;35(1):77-85. doi:10.1007/s10334-021-00982-5

79. Vinogradov E, Sherry AD, Lenkinski RE. CEST: from basic principles to applications, challenges and opportunities. *J Magn Reson.* 2013;229:155-172. doi:10.1016/j.jmr.2012.11.024

80. Lingl JP, Wunderlich A, Goerke S, et al. The value of APTw CEST MRI in routine clinical assessment of human brain tumor patients at 3T. *Diagnostics.* 2022;12(2):490. doi:10.3390/diagnostics12020490